ACS APPLIED MATERIALS & INTERFACES

Research Article

www.acsami.org

A Novel Smart Microsphere with Magnetic Core and Ion-Recognizable Shell for Pb^{2+} Adsorption and Separation

Ying-Mei Liu,[†] Xiao-Jie Ju,*[,†] Yan Xin,[†] Wei-Chao Zheng,[†] Wei Wang,[†] Jie Wei,[†] Rui Xie,[†] Zhuang Liu,[†] and Liang-Yin Chu*[,†,‡]

[†]School of Chemical Engineering, [‡]State Key Laboratory of Polymer Materials Engineering, and Collaborative Innovation Center for Biomaterials Science and Technology, Sichuan University, Chengdu, Sichuan 610065, People's Republic of China

Supporting Information

ABSTRACT: Smart core–shell microspheres for selective Pb^{2+} adsorption and separation have been developed. Each microsphere is composed of a Pb^{2+} recognizable poly(*N*-isopropylacrylamide-*co*-benzo-18-crown-6-acrylamide) (PNB) shell and a magnetic Fe_3O_4 core. The magnetic PNB core–shell microspheres show excellent Pb^{2+} adsorption selectivity among the coexisting Cd^{2+}, Co^{2+}, Cr^{3+}, Cu^{2+}, Ni^{2+}, Zn^{2+}, K^+, and Ca^{2+} ions by forming stable B18C6Am/Pb^{2+} host–guest complexes and exhibit an interesting temperature-dependent Pb^{2+} adsorption. The inner independent magnetic Fe_3O_4 cores enable the Pb^{2+}-adsorbed microspheres with a magnetically guided aggregation to be separated from the treated solution using a remotely controlled manner. The isothermal Pb^{2+} adsorption result fits well with the Freundlich isotherm. The magnetic PNB core–shell microspheres show very fast adsorption of Pb^{2+}, and the adsorption process of Pb^{2+} onto magnetic PNB core–shell microspheres fits well with the pseudo-second-order model. Moreover, Pb^{2+}-adsorbed microspheres can be regenerated by simply increasing the operation temperature and washing with deionized water. The proposed magnetic PNB core–shell microspheres provide a promising candidate for Pb^{2+} adsorbents with selectively separable and efficiently reusable abilities.

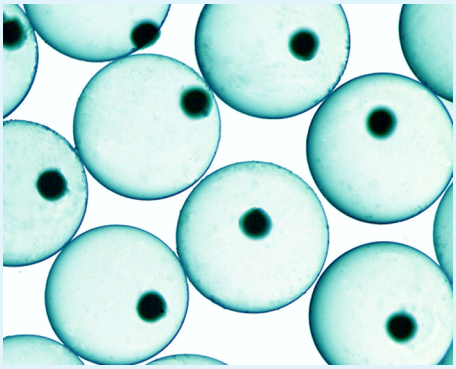

KEYWORDS: *polymer materials, magnetic microspheres, Pb^{2+} adsorption, host–guest chemistry, template synthesis*

1. INTRODUCTION

Lead (Pb^{2+}) is one of the most abundant and toxic heavy metal pollutants. Due to its nonbiodegradability, Pb^{2+} can accumulate in the body from contaminated food and water. Even very low levels of lead intake will cause serious harmful effects on the nervous system, reproductive system, immune system, and liver and kidneys of human beings, especially infants and children.[1,2] However, Pb^{2+} is commonly found in industrial wastewater because of their wide applications in smelting, battery industries, painting, mining, and so on. Therefore, effective removal of Pb^{2+} from industrial wastewater will contribute to environmental sustainability. To achieve that, various technologies, such as chemical precipitation, membrane separation, solvent extraction, ion-exchange and adsorption, have been developed.[3−7] Among them, adsorption is a promising technique because of its high efficiency, easy handling and availability for various adsorbents. In the past few decades, a large number of materials such as activated carbon, chitosan and zeolites, which have high adsorption capacities and are locally available, have been widely used as adsorbents for removal of Pb^{2+}.[7] However, most of these materials show nonspecificity to Pb^{2+} due to their physical adsorption action. These adsorbents can easily become saturated with ubiquitous other species, such as Ca^{2+}, K^+, and so on. In addition, separation and regeneration of these adsorbents from the decontaminated water are extremely challenging. Therefore, design and fabrication of a novel adsorbent with good adsorption capacity and selectivity toward Pb^{2+}, convenient separation, and regeneration from the decontaminated water are of both scientific and technological importance.

18-Crown-6 and its derivatives are one kind of the most promising substances for the design of Pb^{2+} detection and adsorption materials because of their specific Pb^{2+} recognition ability based on the formation of supermolecular host–guest complexes.[8−11] However, most previous investigations are focused on the detection of Pb^{2+} by 18-crown-6 and its derivatives,[12−18] and only a few of them are focused on the selective adsorption of Pb^{2+}.[19−21] A novel Pb^{2+}-imprinted polymer, which is prepared by inverse emulsion polymerization using 4-vinylbenzo-18-crown-6 as a functional monomer, shows good capacity and selectivity toward Pb^{2+}, even in the presence of competitor ions such as Zn^{2+}, Co^{2+}, Ni^{2+}, and Cd^{2+}.[19] Almost 100% removal efficiency for Pb^{2+} from real environmental water samples is achieved. Nevertheless, the size of the Pb^{2+} imprinted polymer is in nanoscale, so separation of the polymer from the decontaminated water is extremely difficult.

Received: March 29, 2014
Accepted: June 4, 2014
Published: June 4, 2014

   dx.doi.org/10.1021/am501919j | *ACS Appl. Mater. Interfaces* 2014, 6, 9530−9542

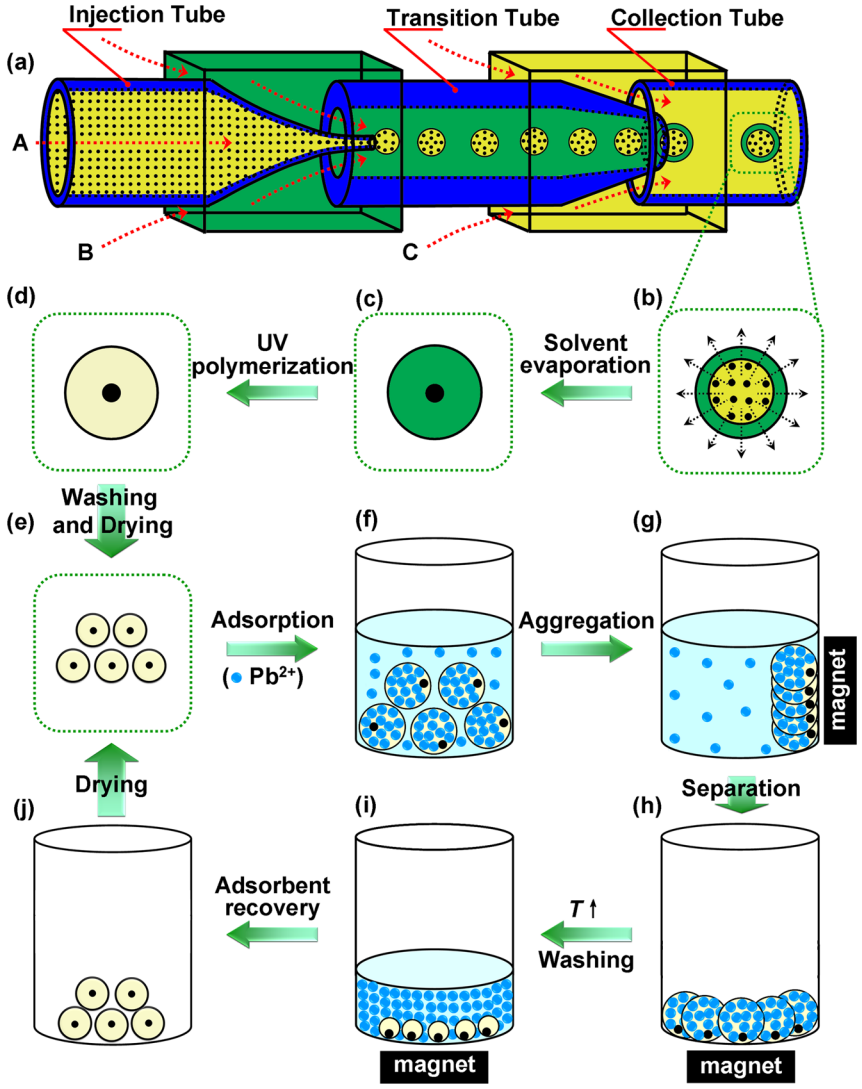

Figure 1. Schematic illustration of the fabrication process of the magnetic PNB core−shell microspheres and the Pb^{2+} adsorption and regeneration processes. (a) Microfluidic device for generating O/W/O emulsion templates, in which A, B, and C stand for the inner, middle, and outer fluid phases, respectively. (b and c) Formation of the magnetic core through solvent evaporation. (d) Fabrication of the magnetic PNB core−shell microspheres through UV-initiated polymerization of the emulsion templates. (e) Purification and dehydration of the magnetic PNB core−shell microspheres by washing and freeze-drying. (f) Adsorption of Pb^{2+} onto the magnetic PNB core−shell microspheres. (g and h) Separation of the adsorbents from the decontaminated solution via magnetic-induced aggregation. (i and j) Removal of the adsorbed Pb^{2+} from the microspheres and regeneration of the adsorbents by increasing environmental temperature and washing with deionized water.

Moreover, HNO_3 (2 mol L^{-1}) implemented in the desorption process may further cause acid pollution. A Pb^{2+} recognition gating membrane has been successfully fabricated by grafting thermoresponsive poly(*N*-isopropylacrylamide) (PNIPAM)[22−24] based copolymers containing 18-crown-6 units onto the pore surfaces of porous membranes.[20] This gating membrane can be used in water treatment for selective detection and removal of trace Pb^{2+}. However, its preparation needs two steps. A thermo- and Pb^{2+}-responsive hydrogel has been fabricated by copolymerization of *N*-isopropylacrylamide (NIPAM) and benzo-18-crown-6-acrylamide (B18C6Am) monomers directly.[21] The poly(NIPAM-*co*-B18C6Am) hydrogel exhibits interesting Pb^{2+}-responsive and temperature-dependent Pb^{2+}-adsorption behaviors. However, the large volumes of the bulk hydrogels restrict their practical applications in Pb^{2+}-contaminated microenvironments. Furthermore, the small specific surface areas of the bulk hydrogels leads to slow Pb^{2+} adsorption and response rates. On the contrary, as microspheres have large specific surface areas, the adsorption and response rates of microspheres toward Pb^{2+} are much faster than the bulk hydrogels. Therefore, it is crucial to develop microsize adsorbents or microspheres with selective and rapid Pb^{2+} adsorption ability, convenient separation, and easy regeneration function.

Recently, the utilization of magnetic materials for wastewater treatment has received much attention due to the advantages of the convenience of magnetic separation and good biocompatibility.[25−41] Various magnetic materials are fabricated by coating magnetic particles with inorganic materials, such as multiwalled carbon nanotubes,[31] porous carbon,[32] and manganese oxide,[33] or with organic materials containing carboxyl groups,[34−38] amine groups,[38] or thiol groups.[34,38−40] However, their adsorption of heavy metal ions is based on either the inorganic shell with large specific surface area, hollow structure, and nonspecific binding sites, or the organic shell with electrostatic attraction between the positive heavy metal ions and the

dx.doi.org/10.1021/am501919j | ACS Appl. Mater. Interfaces 2014, 6, 9530−9542

negative functional groups, which show no selectivity toward Pb^{2+}. A magnetic Pb^{2+}-imprinted polymer (Fe_3O_4@SiO_2−IIP) functionalized with thiol groups for selective removal of Pb^{2+} has been synthesized recently.[41] The Fe_3O_4@SiO_2−IIP has excellent magnetic response and shows higher capacity and selectivity than that of the magnetic nonimprinted polymer (Fe_3O_4@SiO_2−NIP). However, the fabrication process of Fe_3O_4@SiO_2−IIP is extremely complex.[41] Furthermore, HCl solution used in the desorption will bring acid pollution. Although many researchers have reported using magnetic core−shell materials for sensing and adsorption of heavy metal ions, most of the materials have no adsorption selectivity toward Pb^{2+}. Therefore, the development of a novel selective Pb^{2+} adsorption material with convenient magnetic separation is still of practical significance.

Through review of the related reported literatures, the adsorption microsphere material having both excellent Pb^{2+} selectivity and convenient magnetic separation has not been reported yet. In this study, we develop novel core−shell microspheres, each with an Fe_3O_4 magnetic nanoparticles (MNPs) core and an ion-recognizable poly(NIPAM-*co*-B18C6Am) (PNB) shell, which combine the advantages of convenience of magnetic separation and excellent Pb^{2+} selective adsorption. B18C6Am units act as active receptors for Pb^{2+} recognition and adsorption, which can selectively capture Pb^{2+} to form stable 1:1 (ligand/ion) B18C6Am/Pb^{2+} host−guest complexes.[8−11,19−21] PNIPAM networks act as the actuators with thermoresponsive swelling/shrinking configuration change for convenient purification and regeneration of the adsorbents. The inner magnetic core enables the adsorbent with a magnetically guided aggregation to be separated from the decontaminated water, and even with a magnetically guided movement in some Pb^{2+} contaminated microenvironments, using a remotely controlled manner. Core−shell structure guarantees the core and shell materials act independently, and the PNB shell can also protect the magnetic core from leaking.[42,43] The proposed magnetic PNB core−shell microspheres are prepared using oil-in-water-in-oil (O/W/O) double emulsions as templates, which are fabricated from a two-stage microfluidic device (Figure 1a). First, the solid magnetic cores are generated inside the emulsions by solvent evaporation of the inner oil phase (Figure 1b,c). Then, the middle aqueous phase layer (W) is converted to PNB shell through UV-initiated polymerization, from which the magnetic PNB core−shell microspheres, each with an independent magnetic core and an ion-recognizable shell, are formed (Figure 1d). After being washed with deionized water and freeze-dryed, the magnetic PNB core−shell microspheres are used as adsorbents for separation of Pb^{2+} (Figure 1e) from the environment at room temperature (Figure 1f). After the adsorption reaches equilibrium, the microspheres are separated from the decontaminated water by an external magnet (Figure 1g,h). Pb^{2+} ions are then desorbed from 18-crown-6 units by increasing the operation temperature and washing with deionized water repeatedly (Figure 1i), which is caused by the thermo-induced decrease of the inclusion constant of B18C6Am/Pb^{2+} complexes.[9,11] That is to say, the magnetic PNB core−shell microspheres can be regenerated simply by changing the operation temperature and washing with deionized water (Figure 1i,j). Therefore, the proposed magnetic PNB core−shell microspheres can be used as a selectively separable and efficiently reusable Pb^{2+} adsorbent.

2. EXPERIMENTAL SECTION

2.1. Materials. NIPAM (Tokyo Chemical Industry) is purified by recrystallization with a hexane/acetone mixture (v/v, 50/50), and the chemical structure is shown in Figure S1a (Supporting Information). B18C6Am is synthesized according to literature,[44,45] and the chemical structure is shown in Figure S1b (Supporting Information). *N*,*N*′-Methylenebis(acrylamide) (MBA) is used as the cross-linker. 2,2′-Azobis(2-amidinopropane)dihydrochloride (V50) and 2,2-dimethoxy-2-phenylacetophenone (BDK) are used as the water-soluble and oil-soluble initiators, respectively. Pluronic F-127 (Sigma-Aldrich) and polyglycerol polyricinoleate (PGPR 90) (Danisco) are used as the water-soluble and oil-soluble emulsifiers, respectively. 3-(Trimethoxysilyl)propyl methacrylate (TMSPMA) is used to modify Fe_3O_4 MNPs. All other reagents are of analytical grade and used as received. $Pb(NO_3)_2$, $Cd(NO_3)_2$, $Co(NO_3)_2$, $Cr(NO_3)_3$, $Cu(NO_3)_2$, $Ni(NO_3)_2$, $Zn(NO_3)_2$, KNO_3, and $Ca(NO_3)_2$ are dissolved in deionized water as the metal ion solution samples. Deionized water from a Milli-Q Plus water purification system (Millipore) is used throughout the experiments.

2.2. Preparation of Magnetic Nanoparticles. To be well dispersed in ethyl acetate to form the magnetic core in each microsphere, Fe_3O_4 MNPs are modified by TMSPMA via the silanization reaction. TMSPMA-MNPs are prepared according to literature.[43,46] Briefly, after the Fe_3O_4 MNPs are obtained, TMSPMA (6 g) is added into the Fe_3O_4 MNPs drop by drop, and then the solution is mixed at room temperature for 2 h. After the excess TMSPMA is removed, the resultant TMSPMA-MNPs are dispersed in ethyl acetate (100 mL) for further use.

2.3. Microfluidic Device. A capillary microfluidic device is fabricated by assembling glass capillary tubes on glass slides,[47,48] as illustrated in Figure 1a. The inner diameters of the injection, transition, and collection tubes are 550, 250, and 400 μm, respectively. The front ends of the injection tube and transition tube are tapered by a micropuller (Narishige) and then adjusted by a microforge (Narishige) to have inner diameters at 60 and 180 μm, respectively. All cylindrical capillaries are coaxially aligned within the square capillary tubes by matching the outer diameters of the cylindrical tubes to the inner dimensions of the square ones.

2.4. Preparation of Magnetic PNB Core−Shell Microspheres. The magnetic PNB core−shell microspheres are prepared from O/W/O double emulsion templates. Typically, ethyl acetate containing TMSPMA-MNPs is used as the inner oil phase and is ultrasonicated for 15 min before use. NIPAM (1 mol L^{-1}), B18C6Am (0.1 mol L^{-1}), MBA (0.02 mol L^{-1}), Pluronic F-127 (0.5 wt %), and V50 (0.5 wt %) are dissolved in deionized water as the middle aqueous phase (W). Soybean oil containing PGPR 90 (5% (w/v)) and BDK (0.25% (w/v)) is used as the outer oil phase (O). The fluid phases are pumped into the microfluidic device by syringe pumps, and the flow rates of the inner, middle, and outer fluids are Q_A = 500 μL/h, Q_B = 1000 μL/h, and Q_C = 2000 μL/h, respectively. The generated monodisperse O/W/O double emulsions are collected in a collection solution of soybean oil containing PGPR 90 (5% (w/v)) and BDK (0.25% (w/v)). Then, the O/W/O emulsions are kept for 10 min to allow the evaporation of ethyl acetate in the magnetic oil droplets for constructing the solid magnetic core. The middle aqueous phase of the double emulsions is converted into hydrogel networks by UV-initiated polymerization for 15 min in an ice−water bath. A 250 W UV lamp with an illuminance spectrum of 250−450 nm is employed to produce UV light. Cross-linking copolymerization for preparation of poly(NIPAM-*co*-B18C6Am) hydrogel shell of the microspheres is shown in Figure S2 (Supporting Information). The solid magnetic core is encapsulated inside the PNB microgel shell after polymerization. The resultant magnetic PNB core−shell microspheres are washed with isopropanol and deionized water to remove the outer oil phase and unreacted materials. Then the magnetic PNB core−shell microspheres are freeze-dried and preserved as adsorbents for removal of Pb^{2+}. The fabrication process of magnetic PNIPAM core−shell microspheres using as the control group for adsorption of Pb^{2+} in this

work is the same as that of the magnetic PNB core−shell microspheres, but without the addition of B18C6Am.

2.5. Characterization. The morphology and size of TMSPMA-MNPs are characterized by transmission electron microscopy (TEM, JEM-100CX, JEOL). Vibrating-sample magnetometer (7400, Lakeshore) is used to study the magnetic property of the MNPs and the magnetic PNB core−shell microspheres. The formation process of O/W/O double emulsions is observed by an inverted optical microscope (IX71, Olympus) and recorded by a high-speed digital camera (Phantom Miro3, Vision Research). The O/W/O emulsion templates and the resultant core−shell microspheres are observed by an optical microscope (BX61, Olympus), and their size and size distribution are determined on the basis of their optical micrographs using an automatic analytic software. The componential analyses of the samples are characterized by Fourier transform infrared spectroscope (FTIR, IR prestige-21, Shimazu) in the range of 4000−400 cm^{-1} with KBr disc technique. The samples for FT−IR characterization are prepared by a freeze-drying method. Magnetic-induced aggregation of the magnetic PNB core−shell microspheres is performed with a cylindrical NdFeB magnet (size, Ø 4 mm × 10 m; magnetic intensity, 1.2 T). Thermogravimetric analysis measurement (TGA, TG209F1, Netzsch) is performed with a heating rate of 10 °C min^{-1} from 30 to 800 °C under a nitrogen atmosphere. Temperature-responsive diameter changes of the magnetic PNB core−shell microspheres in deionized water and 20 mmol L^{-1} Pb^{2+} solution are observed and recorded by an optical microscope equipped with a thermostatic stage system (TS 62, Instec) and a CCD camera.

2.6. Batch Adsorption Experiments. The ion-adsorption behaviors of magnetic PNB core−shell microspheres in a mixed heavy metal ion solution containing Pb^{2+}, Cd^{2+}, Co^{2+}, Cr^{3+}, Cu^{2+}, Ni^{2+}, and Zn^{2+} with the same initial ion concentration (about 40 mg L^{-1}) and equilibration time are investigated at different pH conditions. The pH values of the mixed ion solutions are adjusted from 2 to 7 using 0.1 mol L^{-1} HCl or NaOH. The weighted magnetic PNB core−shell microspheres (9 g L^{-1}) are added into the containers containing the heavy metal ion solutions with different pH values. Then, these containers are sealed and placed in a shaker bath under 80 rpm to ensure the magnetic core−shell microspheres adsorbents disperse well in aqueous solutions, and the adsorption processes are operated at 25 °C for 12 h. The concentrations of Pb^{2+}, Cd^{2+}, Co^{2+}, Cr^{3+}, Cu^{2+}, Ni^{2+}, and Zn^{2+} before and after adsorption are determined by an inductively coupled plasma optical emission spectrometer (ICP-OES, Spectro Arcos).

For the study of specific and selective Pb^{2+} adsorption of magnetic PNB core−shell microspheres, the adsorption performance of the microspheres in a mixed metal ion solution containing Pb^{2+}, Cd^{2+}, Co^{2+}, Cr^{3+}, Cu^{2+}, Ni^{2+}, Zn^{2+}, K^{+}, and Ca^{2+} at pH 5 has been studied. The initial concentrations of Pb^{2+}, Cd^{2+}, Co^{2+}, Cr^{3+}, Cu^{2+}, Ni^{2+}, and Zn^{2+} are all 40 mg L^{-1}, while the initial concentrations of K^{+} and Ca^{2+} are both 4 mmol L^{-1}, which is about 20 times higher than that of Pb^{2+} (0.2 mmol L^{-1}). The amount of dried magnetic PNB core−shell microspheres in the mixed metal ion solution is 9 g L^{-1}. The ICP-OES method is also used to determine the concentrations of Pb^{2+}, Cd^{2+}, Co^{2+}, Cr^{3+}, Cu^{2+}, Ni^{2+}, Zn^{2+}, K^{+}, and Ca^{2+} before and after adsorption.

An atomic absorption spectroscopy (AAS, SpectrAA 220FS, Varian) method is used to determine the concentrations of Pb^{2+} in the other batch adsorption experiments. The temperature-dependent equilibrium Pb^{2+} adsorption capabilities of magnetic PNB core−shell microspheres are investigated systematically. In the batch adsorption experiments, the weighted magnetic PNB and PNIPAM core−shell microspheres as adsorbents are added into the containers containing the Pb^{2+} solution. The containers are placed in a thermostatic water bath shaker and shaken under 80 rpm at each selected temperature for 12 h.

The equilibrium adsorption capabilities of the microspheres toward metal ions (q_e, mg g^{-1}) and their removal efficiency of metal ions are calculated using the following equations:

$$q_e = \frac{(C_0 - C_e)V}{m} \quad (1)$$

$$\text{Removal percentage} = \frac{C_0 - C_e}{C_0} \times 100\% \quad (2)$$

where C_0 (mg L^{-1}) and C_e (mg L^{-1}) are the concentrations of metal ions in the surrounding solution at the initial time and at equilibrium respectively, m (g) is the weight of microspheres, and V (L) is the volume of metal ion solution.

2.7. Adsorption Kinetics Experiments. $Pb(NO_3)_2$ used in the experiments is a strong electrolyte, so the relationship between the conductivity and concentration of $Pb(NO_3)_2$ solutions is linearly dependent. Thus, the calibration curve for $Pb(NO_3)_2$ solutions between the conductivity and the concentration can be obtained by measuring the conductivity values of $Pb(NO_3)_2$ solutions with a series of known concentrations. The concentration of the $Pb(NO_3)_2$ solution sample can be determined from the calibration curve once the conductivity of the solution sample is measured. Therefore, a conductivity meter (Sevenmulti Neutral Meter, Mettler-Toledo) is used to measure the concentrations of Pb^{2+} in real time during the dynamic Pb^{2+} adsorption experiments. When the magnetic PNB core−shell microspheres as adsorbents (6 g L^{-1}) are added to the Pb^{2+} solution (C_0 = 1 mmol L^{-1}), the measurement is started. The containers are placed in a thermostatic water bath shaker and shaken under 80 rpm at 25 °C.

2.8. Regeneration Studies. Desorption experiments are carried out by increasing temperature and washing with deionized water. After desorption, the magnetic PNB core−shell microspheres are separated by a magnet and then freeze-dried for regeneration.

3. RESULTS AND DISCUSSION

3.1. Preparation and Characterization of Magnetic Nanoparticles (MNPs). The morphology and distribution of the TMSPMA-MNPs are observed by TEM. The mean diameter of the TMSPMA-MNPs is about 10 nm as shown in Figure 2a. The prepared TMSPMA-MNPs disperse quite well in ethyl acetate due to the modification by TMSPMA, which is essential for fabrication of magnetic oil droplets in microfluidic device.

The chemical compositions of TMSPMA, MNPs, and TMSPMA-MNPs are characterized by FT−IR spectrometer (Figure 2b). The characteristic absorption band of Fe_3O_4 at 586.36 cm^{-1} can be found in the spectra of both MNPs (b2) and TMSPMA-MNPs (b3, Figure 2b). The characteristic absorption bands of TMSPMA (b1) also appear in b3, as shown in Figure 2b. For example, absorption bands at 2941.44 and 2845.00 cm^{-1} are attributed to the stretching vibrations of $-CH_2$ group, a strong absorption band at 1722.43 cm^{-1} is attributed to the stretching vibration of the C═O groups. The absorption band at 1633.71 cm^{-1}, corresponding to the vinyl groups of TMSPMA units can be found in the spectrum of the TMSPMA-MNPs, which indicates that the carbon−carbon double bonds (C═C) have been successfully introduced onto the surface of MNPs. The FT−IR results confirm that TMSPMA is successfully coated onto the surface of MNPs via the silanization reaction.

The magnetization hysteresis loop of MNPs at room temperature shows that the saturation magnetization (M_s) of MNPs is 62.77 emu g^{-1} (Figure 2c). The hysteresis and coercivity are almost undetectable, which suggests that the superparamagnetic property of MNPs is satisfactory. Superparamagnetic nanoparticles are of great interest because they do not retain any magnetism after removal of the external magnetic field.

3.2. Fabrication of Monodisperse O/W/O Emulsions and Magnetic PNB Core−Shell Microspheres. Monodisperse O/W/O double emulsions as the templates for

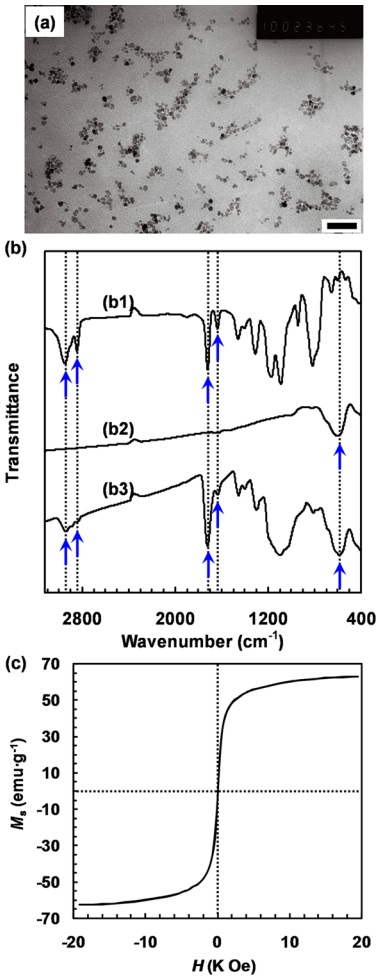

Figure 2. Characterization of magnetic nanoparticles. (a) TEM image of TMSPMA-MNPs. The scale bar is 100 nm. (b) FT−IR spectra of (b1) TMSPMA, (b2) MNPs, and (b3) TMSPMA-MNPs. (c) Magnetization hysteresis loop of MNPs at room temperature.

synthesis of magnetic PNB core−shell microspheres are generated from the microfluidic device (Figure 3a and Movie S1 in the Supporting Information). The magnetic PNIPAM core−shell microspheres without B18C6Am units are also prepared in this work as the control group. The magnetic cores are formed inside the emulsions through the evaporation of inner ethyl acetate. The generated emulsions, which are used as templates for synthesis of magnetic PNB and PNIPAM core−shell microspheres, are shown in Figure 3, panels b and e, respectively. The size of the inner oil droplets greatly decreases after being collected for 10 min. In Figure 3, panels c and f show the optical micrographs of the prepared magnetic PNB and PNIPAM core−shell microspheres in deionized water at 25 °C, respectively. The magnetic core is completely embedded in the hydrogel shell after polymerization of the middle aqueous layer. The size distributions of the emulsion templates and the resultant magnetic PNB and PNIPAM core−shell microspheres dispersed in deionized water at 25 °C are shown in Figure 3, panels d and g, respectively, where d_0, d_1, d_2, and d_3 represent the diameters of the O/W/O double emulsions, the core−shell microspheres, the magnetic oil droplets, and the magnetic cores, respectively. As shown in Figure 3d,g, the sizes of the two kinds of microspheres and their corresponding inner magnetic cores are almost the same, which results from the similar size of the used emulsion templates. It also indicates that the introduction of B18C6Am units has almost no effect on the size of the resulted core−shell microspheres. The average diameter of the magnetic oil droplets is a little smaller than the solid magnetic cores because the magnetic oil droplets are difficult to be focused in the photograph. The coefficient of variation (CV), which is defined as the ratio of the standard deviation of the size distribution to its arithmetic mean, is used to characterize the size monodispersity. The emulsion templates, core−shell microspheres, and inner magnetic cores, whose CV values are all smaller than 5%, all have good monodispersity due to the microfluidic method.

FT−IR analysis is performed to determine the chemical composition of the magnetic PNB core−shell microspheres (Figure 4). The characteristic absorption band of Fe_3O_4 at 586.36 cm^{-1} (curve a) also appears in the spectrum of the magnetic PNIPAM and PNB core−shell microspheres (curves c and d). The characteristic absorption peaks of B18C6Am (curve b), which includes a strong absorption peak at 1514.12 cm^{-1} for C═C skeletal stretching vibration in the phenyl ring and an absorption peak at 1226.73 cm^{-1} for C−O asymmetric stretching vibration in Ar−O−R, also appear in the spectrum of magnetic PNB core−shell microspheres (curve d). The double absorption peaks at 1386.82 and 1367.53 cm^{-1} are characteristic peaks for isopropyl group of PNIPAM (curve c), which also appears in curve d. These results confirm the successful synthesis of the magnetic PNB core−shell microspheres.

3.3. Magnetic Properties of Magnetic PNB Core−Shell Microspheres. The inner magnetic cores enable the prepared core−shell microspheres with a magnetically guided aggregation to be separated from the decontaminated water. The magnetic PNB core−shell microspheres show satisfactory magnetic-responsive aggregation and redispersion properties in deionized water by applying and removing an external magnet, respectively (Figure 5a and Movie S2 in the Supporting Information). The magnetization hysteresis loop of the magnetic PNB core−shell microspheres at room temperature is displayed in Figure 5b. The hysteresis and coercivity are almost undetectable, which suggests that the magnetic PNB core−shell microspheres remain satisfactory superparamagnetic property as a result of the MNPs. The superparamagnetic property of the magnetic PNB core−shell microspheres is critical for their practical application, which prevents them from aggregation and enables them to redisperse rapidly when the magnetic field is removed. The M_s of the magnetic PNB core−shell microspheres is 6.46 emu g^{-1}, which is much lower than that of MNPs (62.77 emu g^{-1}). This significant reduction of M_s is mainly attributed to the presence of nonmagnetic organic components coating on Fe_3O_4 MNPs.

The content of Fe_3O_4 MNPs in the magnetic PNB core−shell microspheres can be determined by TGA. The thermogravimetric curves of Fe_3O_4 MNPs, TMSPMA-MNPs, and magnetic PNB core−shell microspheres characterized in a nitrogen environment are shown in Figure 5c. The weight loss of Fe_3O_4 MNPs is attributed to the gasification of water, and the residual mass percentage is 97.31 wt % at 700 °C. The weight loss of TMSPMA-MNPs is attributed to the gasification of water and decomposition of TMSPMA, and its residual mass percentage is 84.80 wt % at 800 °C. For magnetic PNB core−shell microspheres, the PNB networks and TMSPMA begin to decompose significantly at 300 °C, and the residual mass percentage is 13.49 wt % at 800 °C. Therefore, it can be

dx.doi.org/10.1021/am501919j | ACS Appl. Mater. Interfaces 2014, 6, 9530−9542

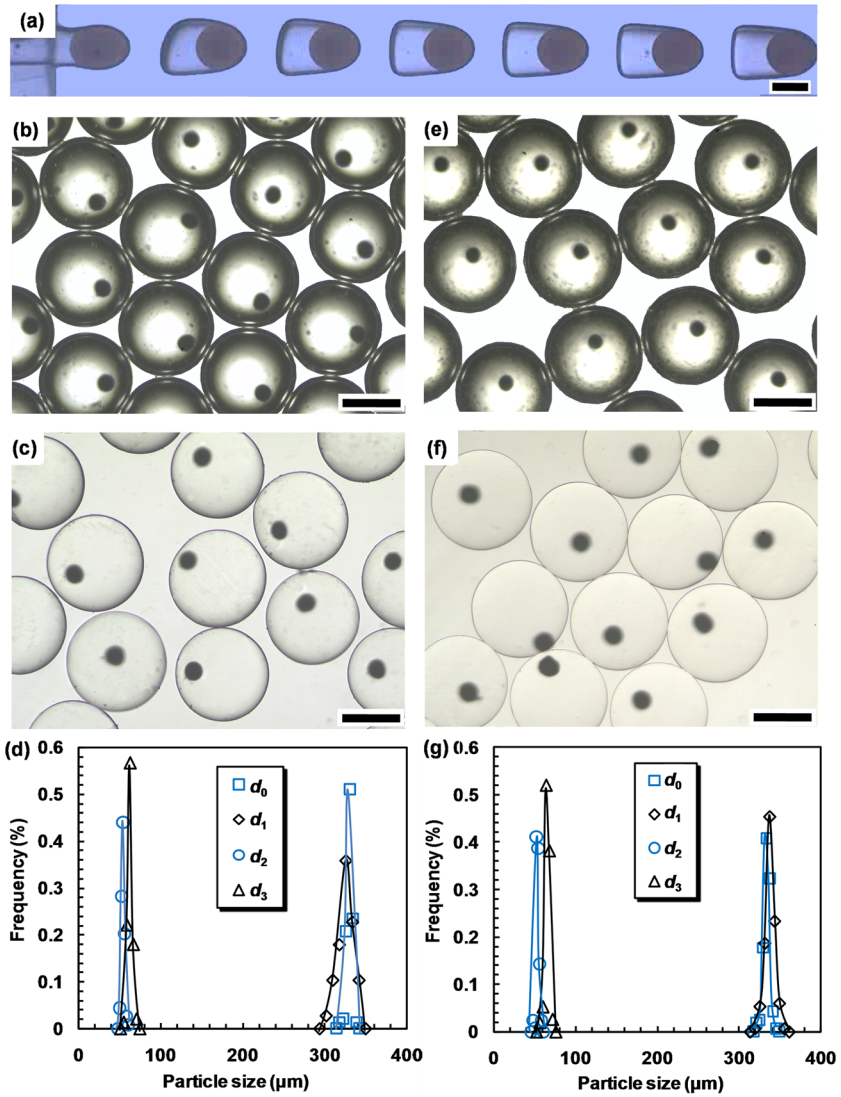

Figure 3. Template synthesis of core−shell microspheres from O/W/O double emulsions. (a) High-speed optical micrograph showing the generation of O/W/O double emulsions in a microfluidic device. Optical micrographs of the emulsion templates used for synthesis of magnetic (b) PNB and (e) PNIPAM core−shell microspheres at about 10 min after formation. The resultant magnetic (c) PNB and (f) PNIPAM core−shell microspheres in deionized water at 25 °C. Size distributions of the magnetic (d) PNB and (g) PNIPAM core−shell microspheres in deionized water at 25 °C and their corresponding emulsion templates, where d_0, d_1, d_2, and d_3 are, respectively, the diameters of the O/W/O double emulsions, the core−shell microspheres, the magnetic oil droplets, and the magnetic cores. Scale bars are 200 μm.

estimated that the content of MNPs embedded in the magnetic PNB core−shell microspheres is about 13.49 wt %.

3.4. Effect of pH on Pb^{2+} Adsorption of Magnetic PNB Core−Shell Microspheres. The ion-adsorption behaviors of magnetic PNB core−shell microspheres in a mixed heavy metal ion solution containing Pb^{2+}, Cd^{2+}, Co^{2+}, Cr^{3+}, Cu^{2+}, Ni^{2+}, and Zn^{2+} with the same initial ion concentration and equilibration time are investigated at different pH conditions. The relationships between the removal efficiencies of various heavy metal ions and the pH values of the mixed heavy metal ion solution are presented in Figure 6. The variation of pH has nearly no obvious effect on removal efficiencies of all heavy metal ions. For Pb^{2+}, there exists only an 8% difference in its removal efficiency over a pH range of 2−7. It is worth noting that the removal efficiencies of magnetic PNB core−shell microspheres toward Pb^{2+} are always much higher than those toward the other metal ions at different pH conditions in the range of 2−7. These results indicate that the magnetic PNB core−shell microspheres can effectively and selectively remove Pb^{2+}, even though the external pH value is changed. The slight decrease of Pb^{2+} removal efficiency with a decrease of pH value from 5 to 2 may be caused by the slight protonation of B18C6Am at lower pH, which results in a reduce of complex ability to Pb^{2+}.[19,49] While the slight decrease of Pb^{2+} removal efficiency with increase of pH value from 5 to 7 may be caused by the formation of lead hydroxide, because Pb^{2+} will precipitate slightly when pH is higher than 5.5.[35] Therefore, the pH value of the aqueous solution in the subsequent experiments is adjusted to 5 to obtain the optimal adsorption.

3.5. Specific and Selective Adsorption of Pb^{2+} by Magnetic PNB Core−Shell Microspheres. To examine the specific and selective Pb^{2+} adsorption of magnetic PNB core−shell microspheres toward Pb^{2+}, the batch adsorption performances of magnetic PNB core−shell microspheres in a mixed metal ion solution containing Pb^{2+}, Cd^{2+}, Co^{2+}, Cr^{3+}, Cu^{2+}, Ni^{2+}, Zn^{2+}, K^{+}, and Ca^{2+} as the contaminated water are

dx.doi.org/10.1021/am501919j | ACS Appl. Mater. Interfaces 2014, 6, 9530−9542

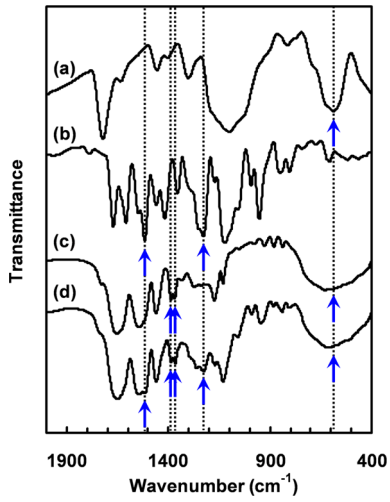

Figure 4. FT−IR spectra of (a) TMSPMA-MNPs, (b) B18C6Am, (c) magnetic PNIPAM core−shell microspheres, and (d) magnetic PNB core−shell microspheres.

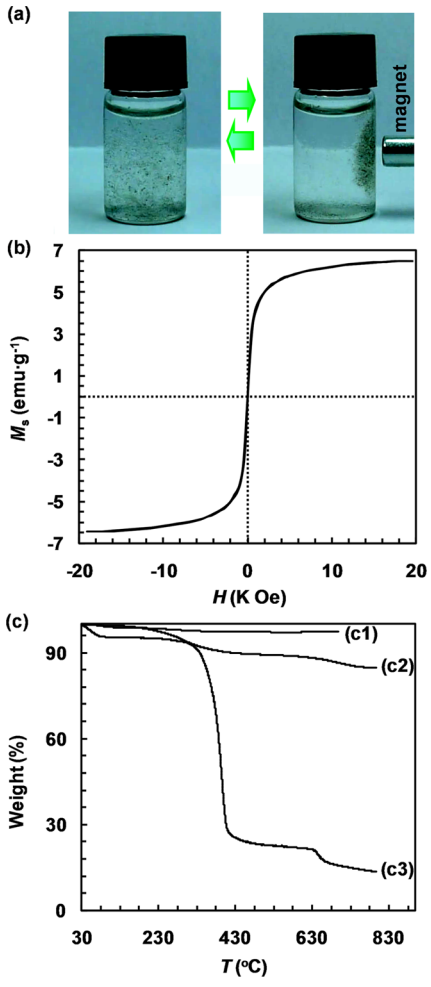

Figure 5. Magnetic properties of magnetic PNB core−shell microspheres. (a) Magnetic-responsive aggregation and redispersion in deionized water by applying and removing an external magnet, respectively. (b) Magnetization hysteresis loop of the magnetic PNB core−shell microspheres at room temperature. (c) Thermogravimetric curves of (c1) MNPs, (c2) TMSPMA-MNPs, and (c3) magnetic PNB core−shell microspheres.

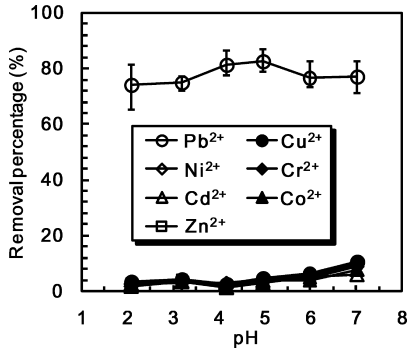

Figure 6. Effects of pH on ion removal efficiencies of magnetic PNB core−shell microspheres in a mixed heavy metal ion solution containing Pb^{2+}, Cu^{2+}, Ni^{2+}, Cr^{3+}, Cd^{2+}, Co^{2+}, and Zn^{2+}. The initial concentrations of the heavy metal ions are all about 40 mg L^{-1}. The amount of PNB microspheres is 9 g L^{-1}, and operation temperature is 25 °C.

investigated, and their removal efficiencies at pH 5 are also studied by the batch adsorption. The removal efficiencies are calculated from the batch adsorption experiment carried out at 25 °C for 12 h. The magnetic PNB core−shell microspheres exhibit a much higher Pb^{2+} removal efficiency than that of the other metal ions, as shown in Figure 7. Pb^{2+} removal efficiency

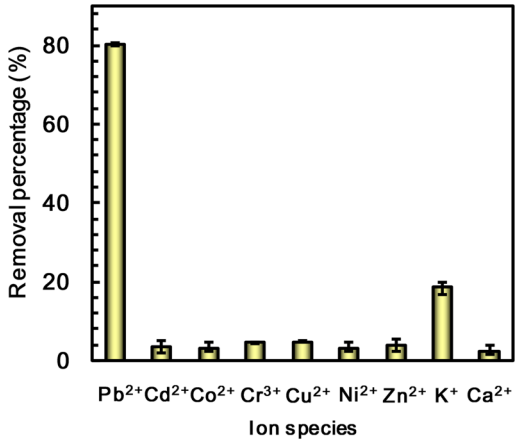

Figure 7. Selective and specific Pb^{2+} adsorption of magnetic PNB core−shell microspheres in a mixed metal ion solution containing Pb^{2+}, Cd^{2+}, Co^{2+}, Cr^{3+}, Cu^{2+}, Ni^{2+}, Zn^{2+}, K^{+}, and Ca^{2+}. The initial ion concentrations of Pb^{2+}, Cd^{2+}, Co^{2+}, Cr^{3+}, Cu^{2+}, Ni^{2+}, and Zn^{2+} are all about 40 mg L^{-1}. The initial ion concentrations of K^{+} and Ca^{2+} are both 4 mmol L^{-1}, which is 20 times higher than that of Pb^{2+} (0.2 mmol L^{-1}). The amount of microspheres is 9 g L^{-1}, the operation temperature is 25 °C, and the pH value of the solution is 5.

is nearly not affected by the addition of Cd^{2+}, Co^{2+}, Cr^{3+}, Cu^{2+}, Ni^{2+}, Zn^{2+}, and Ca^{2+}. Even though the initial concentration of K^{+} (4 mmol L^{-1}) is 20 times higher than that of Pb^{2+} (0.2 mmol L^{-1}), the removal efficiency of Pb^{2+} is still about 4 times higher than that of K^{+}. These results also indicate that the magnetic PNB core−shell microspheres can specifically and selectively capture Pb^{2+} from the mixed ion solution of Cd^{2+}, Co^{2+}, Cr^{3+}, Cu^{2+}, Ni^{2+}, Zn^{2+}, K^{+}, and Ca^{2+} ions. The removal efficiency of K^{+} is higher than that of Ca^{2+}. Such specific adsorption is caused by the formation of stable crown-ether/metal-ion complexes, which is dominated by the size/shape fitting or matching between the host and guest molecules. The B18C6Am receptors in the magnetic PNB core−shell micro-

dx.doi.org/10.1021/am501919j | ACS Appl. Mater. Interfaces 2014, 6, 9530−9542

spheres could selectively capture specific metal ions, whose size fits the cavity size of crown ether well and binds with the cavity tightly and effectively. The complexes' stability constant (log K) of benzo-18-crown-6 with metal ions in water is Pb^{2+} > K^{+} > the other coexisting metal ions.[8−11] Therefore, the magnetic PNB core−shell microspheres exhibit selective Pb^{2+} adsorption based on the formation of stable B18C6Am/Pb^{2+} complexes.[19,20] The magnetic PNB core−shell microspheres in this study show excellent Pb^{2+} adsorption selectivity when compared with the reported Pb^{2+} adsorption materials[7] such as activated carbon, chitosan, and zeolites; magnetic core−shell microspheres coated with inorganic materials, such as multiwalled carbon nanotubes,[31] porous carbon,[32] and manganese oxide;[33] or magnetic core−shell microspheres coated with organic materials containing carboxyl groups,[34−38] amine groups,[38] or thiol groups.[34,38−40]

3.6. Effects of Temperature on Pb^{2+} Adsorption of Magnetic PNB Core−Shell Microspheres. Because the skeleton structure is PNIPAM polymeric network, the magnetic PNB core−shell microspheres exhibit obvious temperature-responsive volume change both in deionized water and 20 mmol L^{-1} Pb^{2+} solution, as shown in Figure 8a. With increasing temperature, the magnetic PNB core−shell microspheres show a thermo-induced shrinking behavior in both deionized water and Pb^{2+} solution. Obviously, the volume phase transition temperature (VPTT) of the magnetic PNB core−shell microspheres shifts to a higher temperature in Pb^{2+}-contained solution ($VPTT_2$) than that in deionized water ($VPTT_1$). Such positive VPTT shift is also caused by the formation of stable B18C6Am/Pb^{2+} complexes. The repulsion among charged B18C6Am/Pb^{2+} complexes and the osmotic pressure within the magnetic PNB core−shell microspheres counteract the shrinkage of the hydrogel networks with the increase of temperature, thereby resulting in the VPTT shifting to a higher temperature.

To investigate the effect of temperature on the adsorption capacity of magnetic PNB core−shell microspheres toward Pb^{2+}, three representative temperatures are chosen from Figure 8a: 25 °C (below $VPTT_1$), 36 °C (between $VPTT_1$ and $VPTT_2$), and 52 °C (higher than $VPTT_2$). The pH values of the Pb^{2+} aqueous solutions are all set at 5. As shown in Figure 8b,c, no matter how the initial concentration of Pb^{2+} or the amount of magnetic PNB core−shell microspheres varies, the highest equilibrium Pb^{2+} adsorption capacity is always obtained at 25 °C at each condition. Such a thermo-induced decrease of Pb^{2+} adsorption capacities of magnetic PNB core−shell microspheres is mainly caused by the decrease of the formation constant of B18C6Am/Pb^{2+} complexes as temperature increases.[9,11] At 25 °C, the formation constant of B18C6Am/Pb^{2+} complex is high, so the cavities of B18C6Am units can capture Pb^{2+} efficiently and tightly. As a result, Pb^{2+} can be effectively removed from the environment. As temperature increases, the formation constant of B18C6Am/Pb^{2+} complex decreases, and thereby, part of captured Pb^{2+} desorbs from the magnetic PNB core−shell microspheres at a higher temperature. The desorbed Pb^{2+} can be squirted out from the microspheres, taking advantage of the thermo-induced dramatic shrinkage of the PNB microspheres. Therefore, the magnetic PNB core−shell microspheres can be regenerated easily by simply increasing the operation temperature and washing with deionized water repeatedly.

3.7. Effect of the Amount of Magnetic PNB Core−Shell Microspheres on Pb^{2+} Adsorption. Pb^{2+} adsorptions

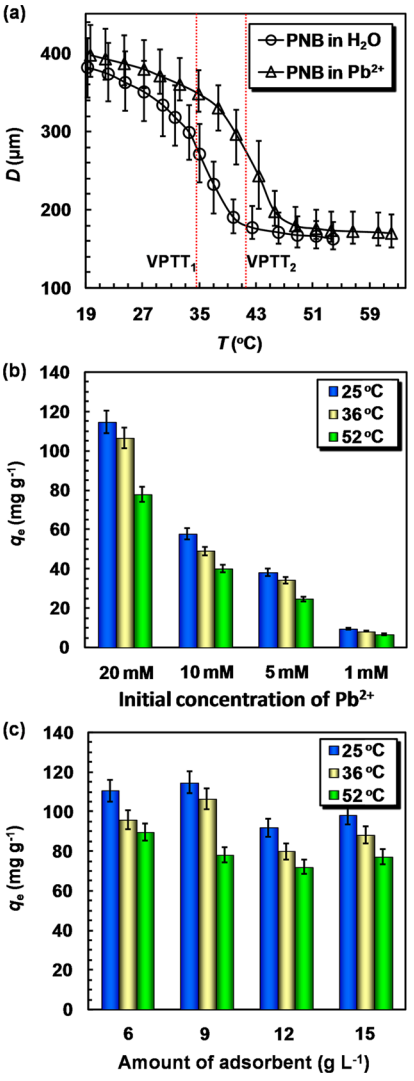

Figure 8. Effects of temperature on the Pb^{2+} adsorption capacity of magnetic PNB core−shell microspheres. (a) Temperature-dependent diameter changes of magnetic PNB core−shell microspheres in Pb^{2+} aqueous solution (20 mmol L^{-1}) and deionized water. (b) Effect of temperature on the Pb^{2+} adsorption capacity with different initial Pb^{2+} concentrations (the amount of adsorbent is 9 g L^{-1}). (c) Effect of temperature on the Pb^{2+} adsorption capacity with different amounts of magnetic PNB core−shell microspheres (C_0 = 20 mmol L^{-1}). The pH values of the solutions are all 5.

with different amounts of microspheres as adsorbents are also performed by the batch adsorption experiments, which are carried out at 25 °C for 12 h, the initial Pb^{2+} concentration is fixed at C_0 = 4200 mg L^{-1}, and the pH value is 5. The equilibrium Pb^{2+} adsorption capacities of magnetic PNB core−shell microspheres with different amounts of adsorbents are shown in Figure 9a, and their corresponding Pb^{2+} removal efficiencies are shown in Figure 9b. When the initial Pb^{2+} concentration is kept constant, the adsorbed amount of Pb^{2+} per unit mass decreases with increasing the amount of adsorbents. However, as the amount of adsorbents increases, more Pb^{2+} can be adsorbed, and therefore, the Pb^{2+} removal efficiency increases. Magnetic PNIPAM core−shell microspheres have the same trend as shown in Figure 9 because of the physical adsorption. More magnetic PNIPAM core−shell microspheres provide more physical adsorption sites. However,

dx.doi.org/10.1021/am501919j | ACS Appl. Mater. Interfaces 2014, 6, 9530−9542

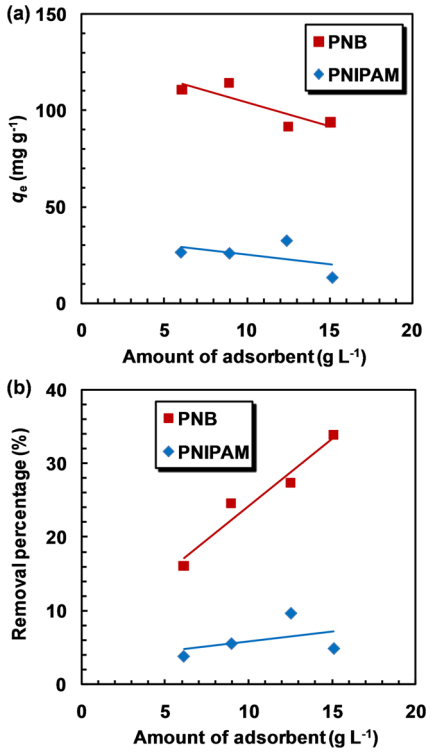

Figure 9. (a) Pb^{2+} adsorption capacity and (b) removal efficiency of magnetic PNB and PNIPAM core–shell microspheres with different amounts (C_0 = 20 mmol L^{-1}). The pH values of the solutions are all 5.

compared to magnetic PNB core–shell microspheres, the Pb^{2+} adsorption capabilities of magnetic PNIPAM core–shell microspheres without B18C6Am units and their corresponding Pb^{2+} removal efficiencies are very small.

3.8. Evaluation of Pb^{2+} Adsorption Behaviors of Magnetic PNB Core–Shell Microspheres. The Pb^{2+} adsorption behaviors of magnetic PNB core–shell microspheres with different initial concentrations of Pb^{2+} are investigated with a fixed amount of microspheres (9 g L^{-1}) at 25 °C for 12 h. The pH values of the Pb^{2+} aqueous solutions are all set at 5. As the initial concentration of Pb^{2+} increases, the Pb^{2+} adsorption capacity of magnetic PNB core–shell microspheres increases obviously, but the corresponding Pb^{2+} removal efficiency decreases, as shown in Figure 10, panels a and b, respectively. Magnetic PNIPAM core–shell microspheres have the same trend. However, the adsorption capabilities and removal efficiencies of magnetic PNIPAM core–shell microspheres without B18C6Am units toward Pb^{2+} are much smaller than those of magnetic PNB core–shell microspheres. Actually, none of the 18-crown-6 units in the magnetic PNB core–shell microspheres in Figure 10 reach the complexation saturation toward Pb^{2+}. Compared with the amount of Pb^{2+} captured on the magnetic PNB core–shell microspheres, the amount of 18-crown-6 units on the microspheres is slightly larger. However, compared with the increase of the initial concentration of Pb^{2+}, the increased amount of captured Pb^{2+} is smaller, so Pb^{2+} removal efficiency decreases. The magnetic PNB core–shell microspheres exhibit a good adsorption capacity toward Pb^{2+}. When the initial concentration of Pb^{2+} is 4200 mg L^{-1}, the adsorption capacity is up to 114.66 mg g^{-1}; however, the Pb^{2+} adsorption capacity of magnetic PNIPAM core–shell is only 25.95 mg g^{-1}.

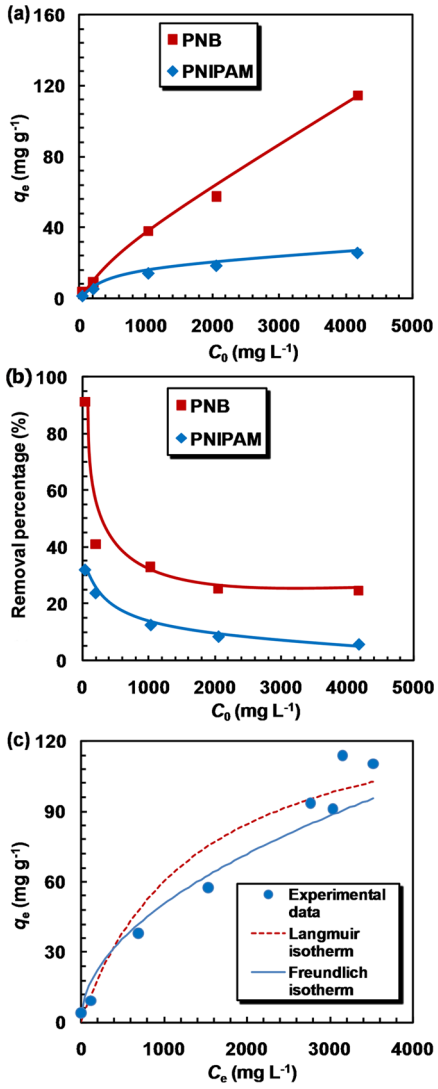

Figure 10. Adsorption capacity of magnetic core–shell microspheres toward Pb^{2+}. The (a) adsorption capacity and (b) removal efficiency of magnetic PNB and PNIPAM core–shell microspheres toward Pb^{2+} with different initial concentrations. (c) Adsorption isotherms of magnetic PNB core–shell microspheres toward Pb^{2+}. Amounts of microspheres are all 9 g L^{-1}, operation temperature is 25 °C, and the pH values of the solutions are all 5.

Freundlich and Langmuir models, which are the most commonly used theoretical models, are applied to fitting the Pb^{2+} adsorption data of magnetic PNB core–shell microspheres. The Freundlich model and the Langmuir model are expressed by eqs 3 and 4, respectively.

Freundlich model:

$$q_e = K_f C_e^{1/n} \quad (3)$$

Langmuir model:

$$q_e = \frac{q_{max} b C_e}{1 + b C_e} \quad (4)$$

where q_e (mg g^{-1}) is the equilibrium Pb^{2+} adsorption capacity, q_{max} (mg g^{-1}) is the maximum Pb^{2+} adsorption capacity, C_e (mg L^{-1}) is the equilibrium concentration of Pb^{2+} in the surrounding solution, K_f and n are the Freundlich constants,

dx.doi.org/10.1021/am501919j | ACS Appl. Mater. Interfaces 2014, 6, 9530–9542

and b is the Langmuir constant. The isotherm constants calculated from the Freundlich and Langmuir equations and their correlation coefficients (R^2) at 25 °C are listed in Table 1.

Table 1. Langmuir and Freundlich Isotherm Constants and Correlation Coefficients of Magnetic PNB Core–Shell Microspheres toward Pb^{2+}

Freundlich			Langmuir		
n	K_f	R^2	q_{max} (mg g^{-1})	b (mL mg^{-1})	R^2
1.9739	1.5356	0.9452	142.8571	0.7233	0.8131

The calculated Freundlich constant n is 1.9739, which indicates that the adsorption of Pb^{2+} using the prepared magnetic PNB core–shell microspheres is favorable.[50] When the Langmuir model is used to describe the adsorption of Pb^{2+}, the calculated q_{max} is 142.8571 mg g^{-1}, which is much larger than the experimental data (114.66 mg g^{-1}). Moreover, the correlation coefficient obtained from the Langmuir isotherm model (R^2 = 0.8131) is lower than that from the Freundlich isotherm model (R^2 = 0.9452), which indicates that the Freundlich isotherm correlates better with the actual experimental data as shown in Figure 10c. It is also estimated that the structure of magnetic PNB core–shell microspheres used for Pb^{2+} adsorption is heterogeneous.[50,51]

3.9. Pb^{2+} Adsorption Kinetics of Magnetic PNB Core–Shell Microspheres. In addition to Pb^{2+} adsorption selectivity and capacity, which are independent of the size of Pb^{2+} adsorbents, it is also favorable to investigate the adsorption rate of magnetic PNB core–shell microspheres toward Pb^{2+}. The dynamic adsorbed amounts of Pb^{2+} by the magnetic PNB core–shell microspheres are calculated using the following equation:

$$q_t = \frac{(C_0 - C_t)V}{m} \tag{5}$$

where q_t (mg g^{-1}) is the adsorbed amount of metal ion at time t; C_0 and C_t (mg L^{-1}) are the concentrations of Pb^{2+} in the surrounding solution at the initial time and that at time t, respectively; V (L) is the volume of Pb^{2+} solution sample; and m (g) is the weight of magnetic PNB core–shell microspheres. In the dynamic Pb^{2+} adsorption experiments, the time-dependent Pb^{2+} adsorption capacity of magnetic PNB core–shell microspheres is also investigated at 25 °C by fixing the initial concentration of Pb^{2+} at 1 mmol L^{-1}, and the pH value of the Pb^{2+} aqueous solution is 5. The amount of microspheres is set at 6 g L^{-1}. There is a sharp increase of Pb^{2+} adsorption in the first 7 min and followed by a slow adsorption process, as shown in Figure 11. The adsorption reaches equilibrium 50 min later (q_e = 7.8 mg g^{-1}). In fact, 90% of Pb^{2+} are adsorbed at the beginning 15 min. Compared with bulk hydrogels, the magnetic PNB core–shell microspheres show faster Pb^{2+} adsorption because the adsorption rate increases with adsorbent size decreasing. Such a rapid adsorption rate in this study is attributed to the large specific surface area of microspheres and good affinity of B18C6Am toward Pb^{2+}.

To further investigate the mechanism of the adsorption kinetics, the pseudo-first-order model (eq 6) and pseudo-second-order model (eq 7) are employed to interpret the experimental data as follows:

$$\ln(q_e - q_t) = \ln q_e - k_1 t \tag{6}$$

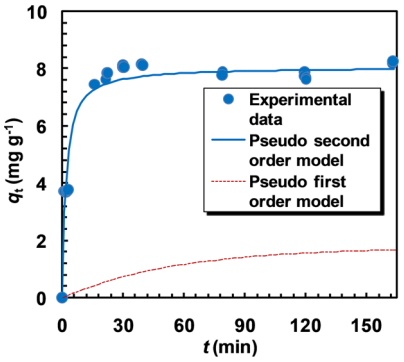

Figure 11. Pb^{2+} adsorption kinetics of magnetic PNB core–shell microspheres at 25 °C (C_0 = 1 mmol L^{-1}, the amount of microspheres is 6 g L^{-1}, and the pH value of the solution is 5).

$$q_t = \frac{q_e^2 k_2 t}{1 + q_e k_2 t} \tag{7}$$

where q_e and q_t (mg g^{-1}) refer to the Pb^{2+} adsorption amount at equilibrium state and at time t, respectively, and k_1 (min^{-1}) and k_2 (g mg^{-1} min^{-1}) are the rate constants of the pseudo-first-order adsorption and pseudo-second-order adsorption models, respectively.

The plots of the two kinetic models are shown in Figure 11. The corresponding kinetic parameters and the correlation coefficients are calculated from the plots and summarized in Table 2. Compared with the pseudo-first-order model, the pseudo-second-order model describes the dynamic Pb^{2+} adsorption much better with a much higher correlation coefficient (R^2 = 0.9981). Moreover, the calculated value of the equilibrium Pb^{2+} adsorption capacity predicted by pseudo-second-order model (8.0710 mg g^{-1}) is closer to the experimental result (7.99 mg g^{-1}). The pseudo-second-order model usually assumes that the rate-limiting step of adsorption is the chemisorption between metal ions and binding sites of adsorbent.[52] Therefore, it can be proved that the adsorption process of Pb^{2+} onto magnetic PNB core–shell microspheres is controlled by the supermolecular host–guest complexation of B18C6Am toward Pb^{2+}.

3.10. Regeneration of the Magnetic PNB Core–Shell Microspheres. Taking into account of cost savings, regeneration of adsorbents is very important. The regeneration of Pb^{2+} adsorbed magnetic PNB core–shell microspheres can be implemented simply by increasing the operation temperature and washing with deionized water. The Pb^{2+} adsorption and regeneration of magnetic PNB core–shell microspheres are performed for five cycles, and the results are shown in Figure 12. The magnetic PNB core–shell microspheres show good thermo-induced reduction of adsorption capacity in each cycle. The Pb^{2+} adsorption capacity at 25 °C only loses 15% after five adsorption–removal cycles. So, it can be inferred that more than 85% of the adsorbed Pb^{2+} ions can be removed from the microspheres by increasing the temperature and washing with deionized water. Compared with the regeneration process of many previously reported Pb^{2+} adsorbents under strong acid solution,[19,33−35,37,41,52] the regeneration of the magnetic PNB core–shell microspheres in this study is much easier and more environmentally friendly. These results indicate that the magnetic PNB core–shell microspheres can be easily and well regenerated and be used repeatedly.

dx.doi.org/10.1021/am501919j | ACS Appl. Mater. Interfaces 2014, 6, 9530−9542

Table 2. Kinetic Model Parameters of Magnetic PNB Core−Shell Microspheres toward Pb^{2+}

	first order			second order		
q (mg g^{-1})	R^2	k_1 (min^{-1})	q_e (mg g^{-1})	R^2	k_2 (g mg^{-1} min^{-1})	q_e (mg g^{-1})
8.25	0.3593	0.0180	1.7773	0.9981	0.0736	8.0710

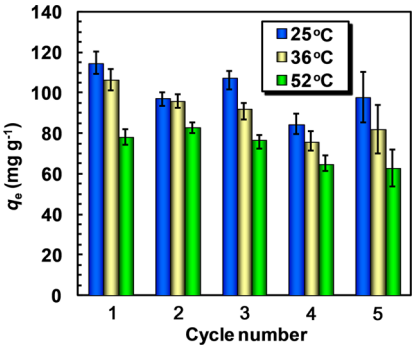

Figure 12. Pb^{2+} adsorption capacities of magnetic PNB core−shell microspheres at different regeneration cycles (C_0 = 20 mmol L^{-1}, the amount of microspheres is 9 g L^{-1}, and the pH values of the solutions are all 5).

4. CONCLUSIONS

In summary, magnetic PNB core−shell microspheres, each with a magnetic core and a Pb^{2+} recognizable poly(NIPAM-*co*-B18C6Am) shell, are successfully fabricated using a microfluidic approach. Although the product output of microfluidic techniques is still limited at the present stage in usual cases, many research groups have already developed integrated microfluidic devices for mass production,[53−56] so the microfluidic techniques have great potential in the practical mass production of emulsions and microparticles for environmental applications on an industrial scale. Using the magnetic PNB core−shell microspheres as novel adsorbents, the pH value of the ion solution shows less impact on the Pb2+ removal efficiency and selectivity. The magnetic PNB core−shell microspheres exhibit selective and rapid Pb^{2+} adsorption through the formation of stable B18C6Am/Pb^{2+} complexes. Due to the inner magnetic core, the Pb^{2+} adsorbed microspheres can be separated from the treated solution through an external magnetic field. The prepared magnetic PNB core−shell microspheres exhibit an interesting temperature-dependent Pb^{2+} adsorption behavior, and their Pb^{2+} adsorption capacities decrease with increasing the temperature, which is caused by the decrease of formation constant of B18C6Am/Pb^{2+} complexes. By simply increasing the operation temperature and washing with deionized water, the Pb^{2+} adsorbed magnetic PNB core−shell microspheres can be easily regenerated. Our smart magnetic PNB core−shell microspheres show great potentials as adsorbents for selective adsorption and separation of Pb^{2+}, which will contribute to the environmental sustainability.

■ ASSOCIATED CONTENT

Supporting Information

High-speed movie showing the generation of O/W/O double emulsions, movie showing magnetic-guided aggregation of the magnetic PNB core−shell microspheres, chemical structures of NIPAM and B18C6Am, and cross-linking copolymerization for preparation of poly(NIPAM-*co*-B18C6Am) hydrogel shell of the microspheres. This material is available free of charge via the Internet at http://pubs.acs.org.

■ AUTHOR INFORMATION

Corresponding Authors

* E-mail: juxiaojie@scu.edu.cn.
* E-mail: chuly@scu.edu.cn.

Notes

The authors declare no competing financial interest.

■ ACKNOWLEDGMENTS

The authors gratefully acknowledge support from the National Natural Science Foundation of China (Grant Nos. 21136006, 21276002, 21322605), the Program for Changjiang Scholars and Innovative Research Team in University (Grant No. IRT1163), the Program for New Century Excellent Talents in University (Grant No. NCET-11-0352), the National High Technology Research and Development Program (863 Program; Grant No. 2012AA021403), and the Foundation for the Author of National Excellent Doctoral Dissertation of China (Grant No. 201163). The authors also thank Mr. G.-L. Cheng in the Analytical and Testing Center of Sichuan University for his help with the AAS measurement.

■ REFERENCES

(1) Kim, H. N.; Ren, W. X.; Kim, J. S.; Yoon, J. Fluorescent and Colorimetric Sensors for Detection of Lead, Cadmium, and Mercury Ions. *Chem. Soc. Rev.* **2012**, *41*, 3210−3244.
(2) Goyer, R. A. Lead Toxicity: Current Concerns. *Environ. Health Perspect.* **1993**, *100*, 177−187.
(3) Lu, P.; Nuhfer, N. T.; Kelly, S.; Li, Q.; Konishi, H.; Elswick, E.; Zhu, C. Lead Coprecipitation with Iron Oxyhydroxide Nano-Particles. *Geochim. Cosmochim. Acta* **2011**, *75*, 4547−4561.
(4) Hegazy, E.-S. A.; Kamal, H.; Khalifa, N. A.; Mahmoud, G. A. Separation and Extraction of Some Heavy and Toxic Metal Ions from Their Wastes by Grafted Membranes. *J. Appl. Polym. Sci.* **2001**, *81*, 849−860.
(5) Das, D.; Sen, K. Species Dependent Aqueous Biphasic Extraction of Some Heavy Metals. *J. Ind. Eng. Chem.* **2012**, *18*, 855−859.
(6) Pehlivan, E.; Altun, T. Ion-Exchange of Pb^{2+}, Cu^{2+}, Zn^{2+}, Cd^{2+}, and Ni^{2+} Ions from Aqueous Solution by Lewatit CNP 80. *J. Hazard. Mater.* **2007**, *140*, 299−307.
(7) Babel, S.; Kurniawan, T. A. Low-Cost Adsorbents for Heavy Metals Uptake from Contaminated Water: A Review. *J. Hazard. Mater.* **2003**, *97*, 219−243.
(8) Zhang, B.; Ju, X.-J.; Xie, R.; Liu, Z.; Pi, S.-W.; Chu, L.-Y. Comprehensive Effects of Metal Ions on Responsive Characteristics of P(NIPAM-*co*-B18C6Am). *J. Phys. Chem. B* **2012**, *116*, 5527−5536.
(9) Izatt, R. M.; Pawlak, K.; Bradshaw, J. S.; Bruening, R. L. Thermodynamic and Kinetic Data for Macrocycle Interaction with Cations and Anions. *Chem. Rev.* **1991**, *91*, 1721−2085.
(10) Takeda, Y.; Kohno, R.; Kudo, Y.; Fukada, N. Stabilities in Water and Transfer Activity Coefficients from Water to Nonaqueous Solvents of Benzo-18-crown-6-Metal Ion Complexes. *Bull. Chem. Soc. Jpn.* **1989**, *62*, 999−1003.
(11) Takeda, Y. Thermodynamic Study of Complex Formation of Benzo-18-crown-6 with K^+, $T1^+$, and Pb^{2+} in Water. *J. Inclusion Phenom. Mol. Recognit. Chem.* **1990**, *9*, 309−313.

(12) Xia, W.-S.; Schmehl, R. H.; Li, C.-J.; Mague, J. T.; Luo, C.-P.; Guldi, D. M. Chemosensors for Lead(II) and Alkali Metal Ions Based on Self-Assembling Fluorescence Enhancement (SAFE). *J. Phys. Chem. B* **2002**, *106*, 833−843.
(13) Yu, M.; He, F.; Tang, Y.; Wang, S.; Li, Y.; Zhu, D. Non-Ionic Water-Soluble Crown-Ether-Substituted Polyfluorene as Fluorescent Probe for Lead Ion Assays. *Macromol. Rapid Commun.* **2007**, *28*, 1333−1338.
(14) Holtz, J. H.; Asher, S. A. Polymerized Colloidal Crystal Hydrogel Films as Intelligent Chemical Sensing Materials. *Nature* **1997**, *389*, 829−832.
(15) Holtz, J. H.; Holtz, J. S. W.; Munro, C. H.; Asher, S. A. Intelligent Polymerized Crystalline Colloidal Arrays: Novel Chemical Sensor Materials. *Anal. Chem.* **1998**, *70*, 780−791.
(16) Asher, S. A.; Peteu, S. F.; Reese, C. E.; Lin, M. X.; Finegold, D. Polymerized Crystalline Colloidal Array Chemical-Sensing Materials for Detection of Lead in Body Fluids. *Anal. Bioanal. Chem.* **2002**, *373*, 632−638.
(17) Reese, C. E.; Asher, S. A. Photonic Crystal Optrode Sensor for Detection of Pb^{2+} in High Ionic Strength Environments. *Anal. Chem.* **2003**, *75*, 3915−3918.
(18) Liu, K.; Ji, H.-F. Detection of Pb^{2+} Using a Hydrogel Swelling Microcantilever Sensor. *Anal. Sci.* **2004**, *20*, 9−11.
(19) Luo, X.; Liu, L.; Deng, F.; Luo, S. Novel Ion-Imprinted Polymer Using Crown Ether as a Functional Monomer for Selective Removal of Pb(II) Ions in Real Environmental Water Samples. *J. Mater. Chem. A* **2013**, *1*, 8280−8286.
(20) Liu, Z.; Luo, F.; Ju, X.-J.; Xie, R.; Sun, Y.-M.; Wang, W.; Chu, L.-Y. Gating Membranes for Water Treatment: Detection and Removal of Trace Pb^{2+} Ions Based on Molecular Recognition and Polymer Phase Transition. *J. Mater. Chem. A* **2013**, *1*, 9659−9671.
(21) Ju, X.-J.; Zhang, S.-B.; Zhou, M.-Y.; Xie, R.; Yang, L.; Chu, L.-Y. Novel Heavy-Metal Adsorption Material: Ion-Recognition P(NIPAM-*co*-BCAm) Hydrogels for Removal of Lead(II) Ions. *J. Hazard. Mater.* **2009**, *167*, 114−118.
(22) Scarpa, J. S.; Mueller, D. D.; Klotz, I. M. Slow Hydrogen−Deuterium Exchange in a Non-α-helical Polyamide. *J. Am. Chem. Soc.* **1967**, *89*, 6024−6030.
(23) Katayama, S.; Hirokawa, Y.; Tanaka, T. Reentrant Phase Transition in Acrylamide Derivative Copolymer Gels. *Macromolecules* **1984**, *17*, 2641−2643.
(24) Xia, L.-W.; Xie, R.; Ju, X.-J.; Wang, W.; Chen, Q.; Chu, L.-Y. Nano-Structured Smart Hydrogels with Rapid Response and High Elasticity. *Nat. Commun.* **2013**, *4*, article number 2226.
(25) Xu, P.; Zeng, G. M.; Huang, D. L.; Feng, C. L.; Hu, S.; Zhao, M. H.; Lai, C.; Wei, Z.; Huang, C.; Xie, G. X.; Liu, Z. F. Use of Iron Oxide Nanomaterials in Wastewater Treatment: A Review. *Sci. Total Environ.* **2012**, *424*, 1−10.
(26) Ambashta, R. D.; Sillanpää, M. Water Purification Using Magnetic Assistance: A Review. *J. Hazard. Mater.* **2010**, *180*, 38−49.
(27) Gong, J.-L.; Wang, B.; Zeng, G.-M.; Yang, C.-P.; Niu, C.-G.; Niu, Q.-Y.; Zhou, W.-J.; Liang, Y. Removal of Cationic Dyes from Aqueous Solution Using Magnetic Multi-Wall Carbon Nanotube Nanocomposite as Adsorbent. *J. Hazard. Mater.* **2009**, *164*, 1517−1522.
(28) Wang, C.; Tao, S.; Wei, W.; Meng, C.; Liu, F.; Han, M. Multifunctional Mesoporous Material for Detection, Adsorption, and Removal of Hg^{2+} in Aqueous Solution. *J. Mater. Chem.* **2010**, *20*, 4635−4641.
(29) Deng, Y.; Qi, D.; Deng, C.; Zhang, X.; Zhao, D. Superparamagnetic High-Magnetization Microspheres with an Fe_3O_4@ SiO_2 Core and Perpendicularly Aligned Mesoporous SiO_2 Shell for Removal of Microcystins. *J. Am. Chem. Soc.* **2008**, *130*, 28−29.
(30) Zhang, Y.; Yan, L.; Xu, W.; Guo, X.; Cui, L.; Gao, L.; Wei, Q.; Du, B. Adsorption of Pb(II) and Hg(II) from Aqueous Solution Using Magnetic $CoFe_2O_4$-Reduced Graphene Oxide. *J. Mol. Liq.* **2014**, *191*, 177−182.
(31) Wang, H.; Yan, N.; Li, Y.; Zhou, X.; Chen, J.; Yu, B.; Gong, M.; Chen, Q. Fe Nanoparticle-Functionalized Multi-Walled Carbon Nanotubes: One-Pot Synthesis and Their Applications in Magnetic Removal of Heavy Metal Ions. *J. Mater. Chem.* **2012**, *22*, 9230−9236.
(32) Wang, H.; Yu, Y.-F.; Chen, Q.-W.; Cheng, K. Carboxyl-Functionalized Nanoparticles with Magnetic Core and Mesopore Carbon Shell as Adsorbents for the Removal of Heavy Metal Ions from Aqueous Solution. *Dalton Trans.* **2011**, *40*, 559−563.
(33) Kim, E.-J.; Lee, C.-S.; Chang, Y.-Y.; Chang, Y.-S. Hierarchically Structured Manganese Oxide-Coated Magnetic Nanocomposites for the Efficient Removal of Heavy Metal Ions from Aqueous Systems. *ACS Appl. Mater. Interfaces* **2013**, *5*, 9628−9634.
(34) Zargoosh, K.; Abedini, H.; Abdolmaleki, A.; Molavian, M. R. Effective Removal of Heavy Metal Ions from Industrial Wastes Using Thiosalicylhydrazide-Modified Magnetic Nanoparticles. *Ind. Eng. Chem. Res.* **2013**, *52*, 14944−14954.
(35) Ge, F.; Li, M.-M.; Ye, H.; Zhao, B.-X. Effective Removal of Heavy Metal Ions Cd^{2+}, Zn^{2+}, Pb^{2+}, Cu^{2+} from Aqueous Solution by Polymer-Modified Magnetic Nanoparticles. *J. Hazard. Mater.* **2012**, *211−212*, 366−372.
(36) Wang, L.; Li, J.; Jiang, Q.; Zhao, L. Water-Soluble Fe_3O_4 Nanoparticles with High Solubility for Removal of Heavy-Metal Ions from Waste Water. *Dalton Trans.* **2012**, *41*, 4544−4551.
(37) Badruddoza, A. Z. M.; Shawon, Z. B. Z.; Daniel, T. W. J.; Hidajat, K.; Uddin, M. S. Fe_3O_4/Cyclodextrin Polymer Nanocomposites for Selective Heavy Metals Removal from Industrial Wastewater. *Carbohydr. Polym.* **2013**, *91*, 322−332.
(38) Singh, S.; Barick, K. C.; Bahadur, D. Surface Engineered Magnetic Nanoparticles for Removal of Toxic Metal Ions and Bacterial Pathogens. *J. Hazard. Mater.* **2011**, *192*, 1539−1547.
(39) Tao, S.; Wang, C.; Ma, W.; Wu, S.; Meng, C. Designed Multifunctionalized Magnetic Mesoporous Microsphere for Sequential Sorption of Organic and Inorganic Pollutants. *Microporous Mesoporous Mater.* **2012**, *147*, 295−301.
(40) Shin, S.; Jang, J. Thiol Containing Polymer Encapsulated Magnetic Nanoparticles as Reusable and Efficiently Separable Adsorbent for Heavy Metal Ions. *Chem. Commun.* **2007**, *41*, 4230−4232.
(41) Guo, B.; Deng, F.; Zhao, Y.; Luo, X.; Luo, S.; Au, C. Magnetic Ion-Imprinted and -SH Functionalized Polymer for Selective Removal of Pb(II) from Aqueous Solution. *Appl. Surf. Sci.* **2014**, *292*, 438−446.
(42) Chen, C.-H.; Abate, A. R.; Lee, D.; Terentjev, E. M.; Weitz, D. A. Microfluidic Assembly of Magnetic Hydrogel Particles with Uniformly Anisotropic Structure. *Adv. Mater.* **2009**, *21*, 3201−3204.
(43) Liu, Y.-M.; Wang, W.; Zheng, W.-C.; Ju, X.-J.; Xie, R.; Zerrouki, D.; Deng, N.-N.; Chu, L.-Y. Hydrogel-Based Microactuators with Remote-Controlled Locomotion and Fast Pb^{2+}-Response for Micromanipulation. *ACS Appl. Mater. Interfaces* **2013**, *5*, 7219−7226.
(44) Yagi, K.; Ruiz, J. A.; Sanchez, M. C. Cation Binding Properties of Polymethacrylamide Derivatives of Crown Ethers. *Makromol. Chem., Rapid Commun.* **1980**, *1*, 263−268.
(45) Ungaro, R.; Haj, B. E.; Smid, J. Substituent Effects on the Stability of Cation Complexes of 4′-Substituted Monobenzo Crown Ethers. *J. Am. Chem. Soc.* **1976**, *98*, 5198−5202.
(46) Chen, T.; Cao, Z.; Guo, X.; Nie, J.; Xu, J.; Fan, Z.; Du, B. Preparation and Characterization of Thermosensitive Organic-Inorganic Hybrid Microgels with Functional Fe_3O_4 Nanoparticles as Crosslinker. *Polymer* **2011**, *52*, 172−179.
(47) Chu, L.-Y.; Utada, A. S.; Shah, R. K.; Kim, J.-W.; Weitz, D. A. Controllable Monodisperse Multiple Emulsions. *Angew. Chem., Int. Ed.* **2007**, *46*, 8970−8974.
(48) Utada, A. S.; Lorenceau, E.; Link, D. R.; Kaplan, P. D.; Stone, H. A.; Weitz, D. A. Monodisperse Double Emulsions Generated from a Microcapillary Device. *Science* **2005**, *308*, 537−541.
(49) Srivastava, S. K.; Gupta, V. K.; Jain, S. Determination of Lead Using a Poly(vinyl chloride)-Based Crown Ether Membrane. *Analyst* **1995**, *120*, 495−498.
(50) Jiang, M.-Q.; Wang, Q.-P.; Jin, X.-Y.; Chen, Z.-L. Removal of Pb(II) from Aqueous Solution Using Modified and Unmodified Kaolinite Clay. *J. Hazard. Mater.* **2009**, *170*, 332−339.

(51) Geary, C. D.; Zudans, I.; Goponenko, A. V.; Asher, S. A.; Weber, S. G. Electrochemical Investigation of Pb^{2+} Binding and Transport through a Polymerized Crystalline Colloidal Array Hydrogel Containing Benzo-18-crown-6. *Anal. Chem.* **2005**, *77*, 185−192.
(52) Jiang, N.; Xu, Y.; Dai, Y.; Luo, W.; Dai, L. Polyaniline Nanofibers Assembled on Alginate Microsphere for Cu^{2+} and Pb^{2+} Uptake. *J. Hazard. Mater.* **2012**, *215−216*, 17−24.
(53) Nisisako, T.; Torii, T. Microfluidic Large-Scale Integration on a Chip for Mass Production of Monodisperse Droplets and Particles. *Lab Chip* **2008**, *8*, 287−293.
(54) Nisisako, T.; Ando, T.; Hatsuzawa, T. High-Volume Production of Single and Compound Emulsions in a Microfluidic Parallelization Arrangement Coupled with Coaxial Annular World-to-Chip Interfaces. *Lab Chip* **2012**, *12*, 3426−3435.
(55) Romanowsky, M. B.; Abate, A. R.; Rotem, A.; Holtze, C.; Weitz, D. A. High Throughput Production of Single Core Double Emulsions in a Parallelized Microfluidic Device. *Lab Chip* **2012**, *12*, 802−807.
(56) Amstad, E.; Datta, S. S.; Weitz, D. A. The Microfluidic Post-Array Device: High Throughput Production of Single Emulsion Drops. *Lab Chip* **2014**, *14*, 705−709.